Ecology Letters, (2003) **6**: 919–928 doi: 10.1046/j.1461-0248.2003.00519.x

REPORT

Species richness, endemism and abundance patterns: tests of two fractal models in a serpentine grassland

Jessica L. Green[1]*, John Harte[2] and Annette Ostling[2]
[1]Department of Environmental Science and Policy, University of California, One Shields Avenue, Davis, CA 95616, USA
[2]Energy and Resources Group, University of California, Berkeley, CA 94720, USA
**Correspondence: E-mail: jlgreen@ucdavis.edu*

Abstract

Although scaling relationships that characterize fractal species distributions offer an exciting potential for unification in biogeography, empirical support for fractal theory remains the subject of debate. We synthesize and test multiple predictions of two interrelated fractal models and a null model of random placement using Californian serpentine grassland data describing the spatial location of over 37 000 individually identified plants. The endemics–area relationship and species-abundance distribution recently derived from a community-level fractal property performed poorly because of an inaccurate assumption of homogeneity among species. In contrast, a species-level fractal model that incorporates species-level differences predicted abundances well, but systematically overestimated endemism and predicted a species–area relationship that violated the observed power law. These findings indicate that in order to make predictions based on the existence of a power-law species–area relationship, ecologists need a unifying theory of how the community-level fractal property arises in the presence of species-level distributional differences.

Keywords

Endemics–area relationship, fractals, random placement, self-similarity, serpentine grassland, species-abundance distribution, species–area relationship.

Ecology Letters (2003) 6: 919–928

INTRODUCTION

Power–law relationships often characterize patterns in the spatial distribution of species across ecologically relevant scale ranges (Rosenzweig 1995; Milne 1997; Ritchie & Olff 1999). These scaling relationships, which take the form of $Y \propto M^b$, offer exciting potential for synthesis in biogeography. Power–law relationships are characteristic of self-similar or fractal phenomena. This observation has motivated theoretical developments to describe and link spatial patterns of species richness, range size, turnover, endemism and abundance across a landscape (Harte & Kinzig 1997; Harte *et al.* 1999a, 2001; Lennon *et al.* 2002). This newly unified theoretical framework describing the interrelationships between multiple biogeographical patterns may elucidate underlying mechanisms responsible for the magnitude and variability of biodiversity (Brown *et al.* 2002). Furthermore, fractal theory provides a means of estimating regional and global scale patterns of species richness, endemism and abundance where it is often impractical to census completely, and has been applied to improve extinction rate estimates following habitat loss (Kinzig & Harte 2000).

Despite the promise of these developments, there has been controversy over whether fractal theory adequately predicts observed spatial biodiversity patterns (Harte & Kinzig 1997; Kunin 1998; Finlayson 1999; Harte *et al.* 1999b, 2001; He & Gaston 2000; Kunin *et al.* 2000; Lennon *et al.* 2002; Ostling *et al.* in press). In addition, central aspects of the theory remain to be tested empirically, including a species-abundance distribution that deviates from the commonly assumed lognormal distribution (Harte *et al.* 1999a). This is likely because of the challenge of obtaining complete abundance information for all species in a region where the spatial distribution of species is clearly fractal. Finally, existing tests have examined only one pattern at a time, leaving the question open as to whether or not the proposed theory adequately links multiple biogeographical patterns.

In this paper, we fill in some of these gaps using plant data collected from a serpentine outcrop in northern California. Studies of spatial patterns in serpentine plant communities, including patterns of local vs. regional species richness, endemism, and how species composition changes across a landscape, has provided some important insights to biogeography and conservation biology (Whittaker 1954,

1960; Harrison 1997, 1999a; Wolf 2001; Harrison & Inouye 2002). Serpentine soils are characterized by a distinct flora because they are poor in calcium and nutrients and contain high levels of magnesium and various metals. These harsh soils exclude many species from the surrounding community and support high levels of endemism. Kruckeberg (2002) estimates that 9% of the flora endemic to California are restricted to serpentine soils.

Using Californian serpentine grassland data describing the spatial location of over 37 000 individually identified plants, we test and contrast the predicted biogeographical patterns of three spatially explicit models. The data collected from our study site was well characterized by a power-law species–area relationship, making it worthwhile to test multiple community-level fractal model predictions. We also test multiple predictions of a species-level fractal model that incorporates species-level differences in fractal dimension ignored in the community-level model. Our study includes the derivation of a new prediction, of the endemics–area relationship, from the species-level fractal model. Finally, we contrast the community- and species-level fractal models to a null model of randomly distributed individuals.

FRACTAL MODEL PREDICTIONS

We first review the species-level and community-level fractal properties. Consider a study region of area A_0 that has been repeatedly bisected into similar-shaped patches, such that sampling areas of size $A_i = A_0/2^i$ are formed from the ith bisection. We consider bisections for simplicity, however the species- and community-level fractal properties are equally valid for trisections, quadrasections, etc. as long as the A_i patches are similarly shaped (Ostling *et al.* in press). At spatial scale i, let R_i denote the range size of a species, defined as the total area occupied by the species as measured using presence/absence data from sampling areas of size A_i. In other words, $R_i = W_i A_i$, where W_i is the number of occupied sampling areas of size A_i. For a particular species, let α_i be the probability that if it is found in a randomly chosen patch of area A_{i-1}, then it is found in a particular one of the two patches of area A_i contained in the chosen A_{i-1}-sized patch. It follows that

$$\alpha_i = \frac{W_i}{2 \cdot W_{i-1}} = \frac{R_i}{R_{i-1}}. \quad (1)$$

The distribution of a species is fractal at the *species-level* if the α_i for that species is independent of i, i.e. if $\alpha_i = \alpha$ for all i. Note that the constants α_i can differ from species to species, and that not all species in a community may have fractal spatial distributions. For each fractally distributed species, we refer to α as its 'species-level' fractal parameter. This parameter is related to the box-counting measure of the fractal dimension, D, of the species distribution by $D = 2[1 + \log_2(\alpha)]$ (Lennon *et al.* 2002).

The community-level fractal property is defined in an analogous manner. Again, consider a region of contiguous habitat of area A_0, and the set of species within a broadly defined taxonomic group, or 'community', such as 'birds' or 'plants'. Let $A_i = A_0/2^i$ be the area of patches that are obtained from the region A_0 through i bisections. We next explain the concept of a 'species occurrence'. By a 'species occurrence' at the ith spatial scale we mean simply an instance of a species being present in an A_i cell. Consider now a patch of size A_{i-1} randomly selected from those located within A_0, and a species occurrence randomly chosen from the set of species occurrences in that A_{i-1} patch. We define $\boldsymbol{a_i}$ to be the probability that this species occurrence is present in a particular one of the two patches of area A_i contained in the chosen A_{i-1}-sized patch. It follows that

$$\boldsymbol{a_i} = \frac{2^i \cdot S_i}{2 \cdot 2^{i-1} \cdot S_{i-1}} = \frac{S_i}{S_{i-1}}, \quad (2)$$

where S_i is the mean species richness in patches of size A_i and S_{i-1} is the mean species richness in patches of size A_{i-1}. The distribution of species is self-similar, or fractal, at the community-level if $\boldsymbol{a_i}$ is independent of i, i.e. if $\boldsymbol{a_i} = \boldsymbol{a}$ for all i. We refer to $\boldsymbol{a}$ as the 'community-level' fractal parameter.

Species–area relationship

The community-level fractal property predicts a power-law species–area relationship (Harte *et al.* 1999a). If the community-level fractal property holds, i.e. if the parameter $\boldsymbol{a_i} = \boldsymbol{a}$ is constant across spatial scales spanning the areas A_0 to A_i, it follows from eqn 2 that the expected number of species in area A_i takes the form:

$$S_i = \boldsymbol{a}^i S_0, \quad (3)$$

where S_0 is equal to the total number of species in the study area A_0. By setting $\boldsymbol{a} = 1/2^z$, eqn 3 can be expressed as the power–law form of the species–area relationship:

$$S_i \propto A_i^z. \quad (4)$$

A species–area relationship can also be derived from species-level fractals (Lennon *et al.* 2002). If the distribution of an individual species is fractal across spatial scales spanning the areas A_0 to A_i, the probability that this species is present in a randomly-chosen sampling area A_i within A_0 is $p(A_i) = \alpha^i$. The expected number of species in sampling area A_i, S_i, is the sum, over all species, of the probabilities $p(A_i)$. Hence if each species k in A_0 exhibits the fractal property with its own parameter $\alpha_{(k)}$, the species–area relationship follows

$$S_i = \sum_{k=1}^{S_0} {\alpha_{(k)}}^i, \quad (5)$$

where the dependence on area is reflected in the dependence on the scale *i*. The species-level fractal model, which assumes scale invariant α values, will only satisfy a power-law species–area relationship when $\alpha = \boldsymbol{a}$ for all species. If the condition $\alpha = \boldsymbol{a}$ for all species is violated, then a power-law species–area relationship can hold only if one or more of the S_0 species have scale dependent α values (Harte *et al.* 2001; Ostling *et al.* in press).

Endemics–area relationship

Here we derive a new prediction of the endemics–area relationship under the case of species–level fractals with fractal dimension varying across species. Recall that $1 - \alpha_i$ is the probability that if a species is present in a randomly chosen A_{i-1} sampling area, then it is present in only one of the two A_i formed by bisection of the chosen A_{i-1}. It follows that if a species is self-similarly distributed across the spatial scales spanning from A_0 to A_i, the probability the species is confined (or endemic to) a randomly chosen sampling area A_i within A_0 is $e(A_i) = (1 - \alpha)^i$. The expected number of species endemic to sampling area A_i, E_i, is the sum across all species of the probability $e(A_i)$. Adding in the subscript (k) to denote species yields:

$$E_i = \sum_{k=1}^{S_0} [1 - \alpha_{(k)}]^i. \quad (6)$$

This expression provides the dependence of endemic species richness on area through its dependence on the scale subscript *i*.

Harte & Kinzig (1997) and Harte *et al.* (1999a) derived an endemics–area relationship of the form

$$E_i = S_0(1 - \boldsymbol{a})^i, \quad (7)$$

which yields a power-law dependence of endemics species richness on area with an exponent related to the species–area exponent *z*. Equation 7 was derived under the assumption that the probability $\boldsymbol{a}$ can be applied to the occurrences of species which are endemic down to scale A_{i-1}, a non-random subset of all of the species occurrences at this scale. However, $\boldsymbol{a}$ does not necessarily apply to such non-random subsets even if community-level self-similarity holds. This assumption is slightly more general than, but follows from, assuming $\alpha = \boldsymbol{a}$ for all species (and in this case eqn 7 follows directly from eqn 6). Equation 7 is the community-level fractal model prediction of the endemics–area relationship that we test in this paper.

Estimating species-abundances

The species-level fractal property may be applied to relate the abundance of a species at two different spatial scales (Kunin 1998; He & Gaston 2000; Kunin *et al.* 2000). If a species is self-similarly distributed across spatial scales spanning the areas A_0 to A_i, it follows from eqn 1 that $R_i = \alpha^i R_0$, or $W_i A_i = \alpha^i A_0$, where W_i is the number of occupied sampling areas of size A_i. If the average density for the occupied sampling areas of size A_i is μ_i, then the expected density (or abundance) in A_0 is $\mu_0 = \mu_i W_i$, or:

$$\mu_0 = \left[\frac{\alpha^i A_0}{A_i}\right] \mu_i. \quad (8)$$

With an estimate of the species-level self-similarity parameter, α, the abundance of a species at the largest sampling area (A_0) may be predicted by collecting abundance data (μ_i) for that species at smaller sampling areas (A_i). In this paper, we test the species-level fractal model prediction that the abundance of each species scales according to eqn 8.

In earlier work, Harte *et al.* (1999a) asserted that if a community of species was characterized by a power-law species–area relationship, then the solutions to the following recursion relation describes the distribution of abundances across species (i.e. the species-abundance distribution) for that community at each scale:

$$P_{i-1}(n) = 2(1 - \boldsymbol{a})P_i(n) + (2\boldsymbol{a} - 1)\sum_{k=1}^{n-1} P_i(k)P_i(n-k). \quad (9)$$

Here, we more clearly state the meaning of eqn 9 and the assumptions required to derive eqn 9. The solution to eqn 9 describes the fraction of species occurrences in all the A_i that have abundance *n*. Or, stated in another way, $P_{i-1}(n)$ is the probability that a species occurrence, chosen at random from all species occurrences on the landscape at the $i - 1$ scale, will have abundance *n*. Equation 9 will hold for this definition of $P_{i-1}(n)$ if one assumes that the community-level fractal property holds, and makes the following two additional assumptions: 1) the probability $\boldsymbol{a}$ applies to subsets of the species occurrences in A_i which all consist of a particular abundance *n*, and 2) the probability for a species to have *n* individuals in an A_i is independent of the abundance of that species in the adjacent A_i contained in the A_{i-1}. Assumption 1) is less restrictive than, but holds under, the assumption that the probability $\boldsymbol{a}$ applies to all species occurrences in the A_{i-1}. This more restrictive assumption clearly has the consequence that every species will be fractally distributed with the same self-similarity parameter $\alpha = \boldsymbol{a}$. Equation 9 is the community-level fractal model abundance prediction we test in this paper.

METHODS

Field data were collected from serpentine substrates at the Donald and Sylvia McLaughlin University of California

Natural Reserve (latitude 38°51′N, longitude 123°34′W) in northern Napa and southern Lake Counties, 120 km north of San Francisco, CA, USA. The soils, geology, flora, and vegetation of this area are described by the University of California-Davis Natural Reserve System (UCD-NRS) (2003). Within the reserve, species-abundance data were collected from a grassland plant community at a site called Little Blue Ridge. Little Blue Ridge is one of the undisturbed sites that has been used in regional scale studies examining the impacts of grazing, fire, and invasion on plant diversity in serpentine vs. non-serpentine substrates (Harrison 1999b; Harrison *et al.* 2003). This particular site was chosen because there were few rhizomatous grasses; thus, it was possible to distinguish individuals of every vegetative species. The plants at this site are very small, hence an area 100 m^2 has on the order of a hundred thousand individuals. At the site, we laid out one square 64 m^2 plot. The plot was gridded into 256 0.25 m^2 sampling areas, and the total abundance of each species in every 0.25 m^2 sampling area was recorded. These data were collected in early May to late-July 1998. By sampling throughout this time period, it was possible to sample all plant species while they were flowering. Plants were identified with the help of an expert regional botanist (Joseph Callizo). Species nomenclature in this paper follows that of Hickman (1993).

To test the community-level fractal model predictions we assumed $\boldsymbol{a} = 1/2^{\chi}$, with χ equal to the slope of the log–log species–area relationship at the Little Blue Ridge. To plot the species–area relationship at the site we applied the familiar method of calculating the average species richness, S_i, in non-overlapping equal shaped (square) sampling areas (Condit *et al.* 1996). To test the species-level fractal model predictions requires estimating α for each species at the site. Similar to earlier studies (Kunin 1998; Lennon *et al.* 2002), we applied the box-counting method to estimate α from the slope of the range–area relationship (or scale–area curve) plotted for equal shaped (square) sampling areas. Hence, for each species, we assumed $\alpha = 1/2^{\gamma'}$, with γ' equal to the slope of $\log(R_i)$ vs. $\log(A_i)$. Note that the slope $\gamma' = 1 - \frac{D}{2}$, where D is the box-counting dimension of the species' distribution. As discussed by Kunin *et al.* (2000) the box-counting method is sensitive to the effects of 'grid saturation' or 'dilution'. For sufficiently large sampling areas, the range–area relationship is likely to either level off with a slope of zero (grid saturation) or rise with a slope of one (grid dilution). The former occurs if the species is relatively widespread throughout A_0 because once the species is found in every one of the A_i cells, then it will be found in every one of the larger aggregation of those cells, and R_i will be constant with increasing sampling area A_i. The latter occurs if the species is relatively confined to a portion of A_0; for example if a species is only found in the upper left octant of A_0 then for $A_i > A_0/8$, R_i will increase linearly with A_i. To compensate for these effects, we omitted from our range–area curves data collected at spatial scales reaching either of these limits.

We have completely sampled the site, and hence know the true endemic richness and species richness values at each scale for the site. What we need to know in order to accept or reject our fractal and random placement models is how much the mean total and endemic species richness can diverge from their expected values in finite landscapes for which each of these models holds. Hence, to test the fractal and random placement model predictions, we simulated 1000 landscapes for each model. Fractal model landscapes were simulated using the estimated probabilities $\boldsymbol{a}$ and α, and random placement model landscapes were simulated using the observed number of individuals of each species at Little Blue Ridge. In creating these landscapes, we applied the probabilities $\boldsymbol{a}$ and α to each and every species occurrence, regardless of the location of other species occurrences that were already determined. It is possible that each of the fractal properties could arise in some more complicated manner, in which the locations of species occurrences are dependent on one another.

For each simulation, we calculated a statistic analogous to those commonly used in the analyses of spatial point patterns (Diggle 1983; Plotkin 2000):

$$k_{\text{simulation}} = \sum_i [\log(1 + Y_{i,\,\text{model}}) - \log(1 + Y_{i,\,\text{simulation}})]^2, \tag{10}$$

where $Y_{i,\,\text{model}}$ and $Y_{i,\,\text{simulation}}$ are the predicted and simulated values of mean species or endemic species richness at spatial scale i. In the case of the random placement model, we assumed $Y_{i,\,\text{model}}$ was equal to the mean value of $Y_{i,\,\text{simulation}}$ across all 1000 simulations. For each model, the transformation $\log(1 + Y_i)$ yielded the highest level of homoscedasticity in the simulation residuals. We compared the values of $k_{\text{simulation}}$ to:

$$k_{\text{observed}} = \sum_i [\log(1 + Y_{i,\,\text{model}}) - \log(1 + Y_{i,\,\text{observed}})]^2. \tag{11}$$

If k_{observed} is greater than a high percentage of the $k_{\text{simulation}}$ values, one may conclude that the model does not describe the observed data. We used one minus the percentage of simulations where $k_{\text{observed}} > k_{\text{simulation}}$ as the P-value of our tests.

To test the community-level fractal model recursion relation (eqn 9), we calculated the probabilities $P_i(n)$ assuming $\boldsymbol{a} = 1/2^{\chi}$. In addition, we assumed that eqn 9 can be applied iteratively all the way from the scale $i = m$ at which a species has an average of one individual per A_m it

occupies [i.e. at which $\mu_m = 1$ and hence $P_m(1) = 1$], up to the spatial scales at which we measured the distribution of individuals. To calculate m, we set $\mu_m = (N_0/S_0)/(2\boldsymbol{a})^m$, where N_0/S_0 is the average number of individuals per species, and $(2\boldsymbol{a})^m$ is the average number of A_m it occupies, and solved for m. The result, using the observed values ($\boldsymbol{a} = 0.86$; $S_0 = 24$; $N_0 = 37\,182$) reported below, was $m = 13.5$, which we rounded to $m = 13$. Hence we assumed $P_{13}(1) = 1$. However, numerical investigation indicates that beyond several doublings of spatial scale, the shape of the predicted distribution $P_i(n)$ is insensitive to plausible variation in the small scale distribution $P_m(n)$. For example, we found very little difference in the predicted values for $P_i(n)$ at large spatial scales (small i) when the observed $P_8(n)$ was used as a scale boundary condition instead.

To test the species-level fractal model prediction of species abundances in A_0 we assumed that the fitted α of each species was constant across spatial scales spanning the areas $A_0 = 64$ m^2 to $A_{13} \approx 0.008$ m^2 and that $\mu_{13} = 1$ for each species. For both the community- and species-level fractal model predictions, we applied the δ-corrected Kolmogorov–Smirnov goodness of fit test (Zar 1999) to test the hypothesis that the observed and predicted species-abundance distributions were equal. Finally, for both models, we compared the observed and predicted evenness in A_0 using the well established Pielou metric J' (Pielou 1975); J' ranges from 1 to 0, representing changes in distribution of abundances from even to uneven.

RESULTS

There were a total of 24 species and 37 182 individuals at the site ($S_0 = 24$, $N_0 = 37\,182$, Table 1). Table 2 summarizes the performance of each model. The observed species–area relationship was well modelled by a power-law (Fig. 1), and the predicted community-level fractal model species–area relationship (eqn 3) fit the data ($P > 0.67$). A weighted linear regression of $\log_{10}(S_i)$ vs. $\log_{10}(A_i)$ yielded $r^2 > 0.999$, with slope $z = 0.21$, corresponding to an estimated community-level self-similarity parameter $\boldsymbol{a} = 1/2^z = 0.86$. Both the species-level fractal model (eqn 5) and the random placement model predicted species–area relationships were significantly different from the observed ($P < 0.001$). Examples of the log–log range–area relationships used to estimate the species-level fractal parameters α are illustrated in Fig. 2.

The random placement model most closely predicted the observed endemics–area relationship at Little Blue Ridge (Fig. 3; $P > 0.999$). While the community-level fractal model (eqn 7) systematically underestimated endemic species richness, the species-level fractal model (eqn 6) systematically overestimated endemic species richness.

Table 1 Species list

	Abundance
Asteraceae	
Ancistrocarphus filagineus	30
*Calycadenia pauciflora**	3095
Grindelia camporum	120
Lasthenia californica	6
Microseris douglassi	1418
Microseris elegans	50
Unidentified yellow composite	1
Unidentified tarweed	1759
Brassicaceae	
Athysanus pusillus	2
Lepidium nitidum	112
Caryophyllaceae	
Minuartia douglasii	272
Fabaceae	
Lotus humistratus	7
Lupinus bicolor	2
Liliaceae	
Allium serra	5989
Dichelostemma capitatum	49
Pinaceae	
Pinus sabiniana	1
Plantaginaceae	
Plantago erecta	4827
Poaceae	
Bromus hordeaceus†	885
Bromus madritensis†	6990
Elymus elymoides	13
Vulpia microstachys	10792
Polemoniaceae	
Gilia sinistra	617
Polygonacae	
Eriogonum nudum	139
Unidentified	
Sawtoothed leaves	6

*Serpentine endemic.
†Alien.

Although the observed endemics–area relationship was significantly different than that predicted by either of the fractal-models ($P < 0.001$), the species-level fractal model, which incorporates interspecific variation in the α's, more successfully captured the observed trends in the slope of the endemics–area relationship when plotted on log–log axes.

At every spatial scale, the community-level fractal model recursion relation (eqn 9) markedly underestimated the frequency of species occurrences with abundance below the modal value (Fig. 4a), and the observed and predicted species-abundance distributions were significantly different ($P < 0.001$). Using Monte-Carlo simulations, we generated a list of abundances for 24 species according to the probability distribution $P_0(n)$ (eqn 9). The mean predicted

	Community-level fractal model	Species-level fractal model	Random model
Species–area relationship	Not rejected	Rejected*	Rejected*
Endemics–area relationship	Rejected*	Rejected*	Not rejected
Abundance	Rejected*	Not rejected	Not applicable

Table 2 Summary of model prediction performance

*Significance level $P < 0.001$.

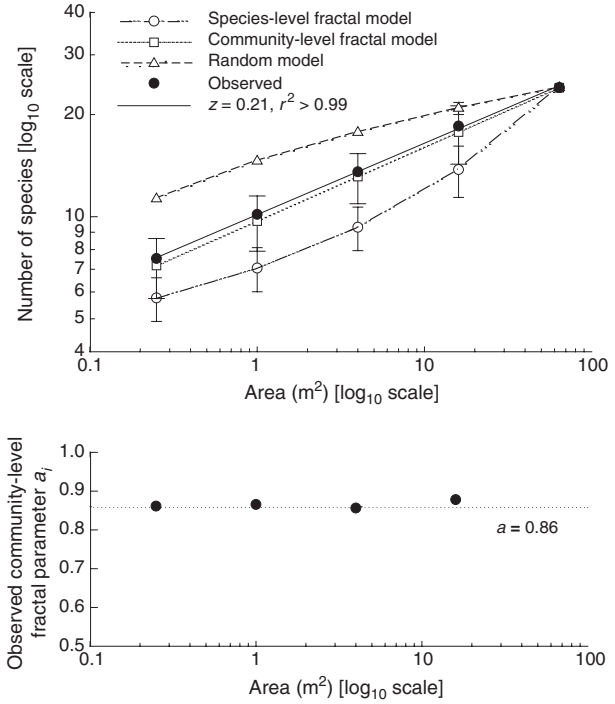

Figure 1 (a) A comparison of the observed and predicted species–area relationships at Little Blue Ridge. The observed species-area curve is well fit by a power-law and hence agrees with the community-level self-similarity model prediction. The solid line is a weighted least squares regression (weights correspond to sample size) through the observed data, yielding $r^2 > 0.999$ and slope of $z = 0.21$. For each model, error bars represent 95% confidence intervals calculated from 1000 simulated landscapes; error bars smaller than symbols are not plotted. At the largest sampled spatial scale, the observed data and each model agree, as they must. At smaller spatial scales, the observed data lie outside the 95% confidence interval for both the species-level self-similarity model and for the random placement model. (b) The observed community-level fractal parameter $\boldsymbol{a}_i = \sqrt{S_i/S_{i-2}}$ was relatively constant with spatial scale i. Self-similarity predicts $\boldsymbol{a} = 1/2^{0.21} = 0.86$, represented by the dashed line.

evenness across 1000 simulations ($J' = 0.98$) was much greater than the observed ($J' = 0.63$).

The species-level fractal model predictions (eqn 8) were in close agreement with the observed abundances in A_0, and we were unable to reject the hypothesis that the observed and predicted species-abundance distributions were equal (Fig. 4b; $P > 0.50$). Although there was a tendency to overestimate the species' abundances (Fig. 4c), the resulting evenness ($J' = 0.66$) was in close agreement with the observed.

DISCUSSION

The species–area relationship is one of the most widely discussed patterns in ecology. Although certain ecological assemblages are poorly characterized by a power-law species–area relationship (Plotkin *et al.* 2000; Crawley & Harral 2001), the power-law is a good descriptor of species richness scaling patterns for many habitats and taxonomic groups (Rosenzweig 1995). Recently, Harte and colleagues developed theory that would enable ecologists to predict spatial patterns of endemism and species abundance across a landscape as a function of one parameter, the power-law species–area relationship exponent z (Harte & Kinzig 1997; Harte *et al.* 1999a). Armed with complete abundance data from a site well characterized by a power-law species–area relationship, our study is the first to test these predicted patterns of endemism and abundance. Our results show that the hypothesized relationships poorly describe the observed patterns, and we conclude that this is because of inaccurate assumptions involved in their derivation. The community-level fractal model predictions of Harte & Kinzig (1997) and Harte *et al.* (1999a) involved the assumption that the spatial distribution of each species is fractal with the same species-level fractal parameter α, and this unrealistic assumption of homogeneity among species is why these predictions performed poorly. Our findings indicate that in order to make predictions based on the existence of a power-law species–area relationship, ecologists need a unifying theory of how the community-level fractal property arises in the presence of species-level distributional differences.

Our aim in testing the species-level fractal model was to explore the degree to which accounting for differences in species-level spatial distributions influenced the predicted patterns of species richness, endemism and abundance. The distribution of observed values of the species-level fractal parameter α (and hence the fractal dimension D) at Little Blue Ridge was much more uniform than those reported by (Lennon *et al.* 2002) for Alaskan trees and British grasses. This wider range of conspecific clustering may reflect the larger number of growth forms present at the site, which

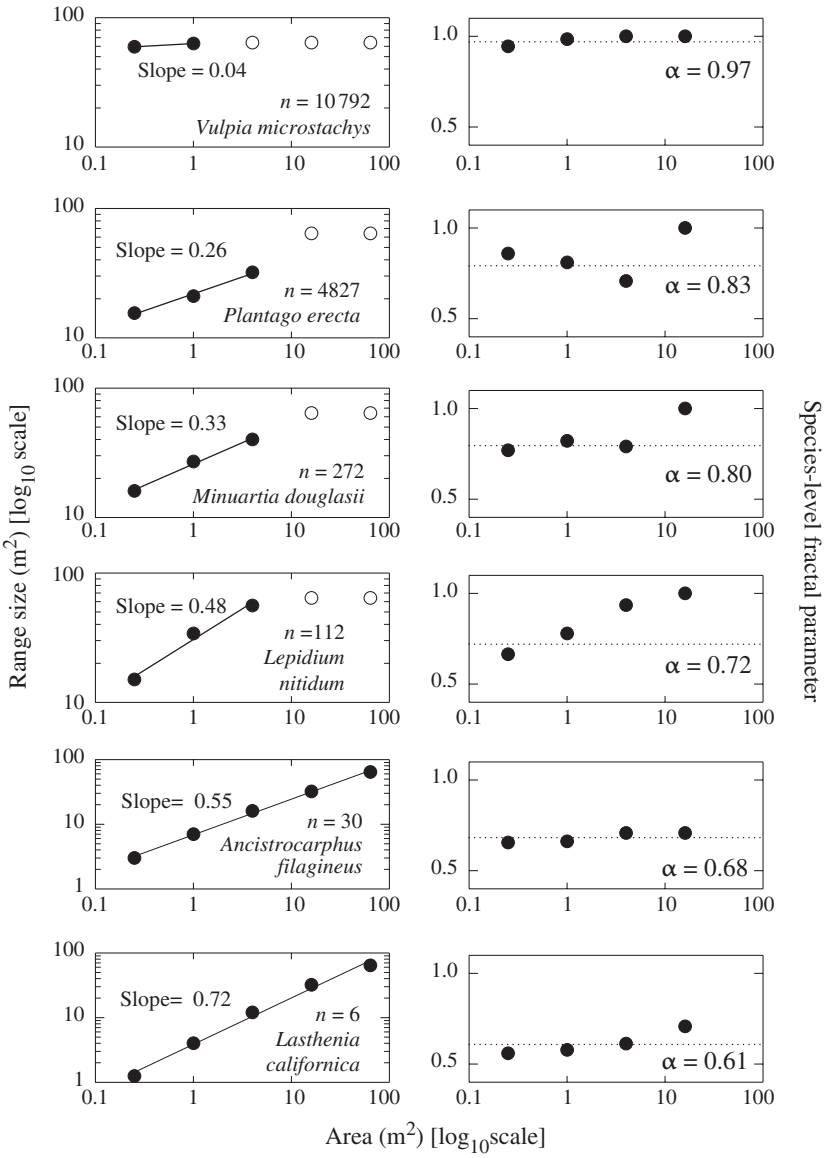

Figure 2 Left panels illustrate a sample of the observed range–area relationships (scale-area curves) at Little Blue Ridge for relatively high, intermediate, and low abundance flora (open circles). Solid circles represent the range–area relationships prior to grid saturation. The slope of the solid line (y') is the least squares regression used to estimate the species-level fractal parameter $\alpha = 1/2^{y'}$. Right panels illustrate the corresponding species-level fractal parameters $\alpha_i = \sqrt{R_i/R_{i-2}}$ across the spatial scales $i = 8$ ($A_8 = 0.25$ m^2) through $i = 2$ ($A_2 = 16$ m^2). The dashed line represents the species-level fractal parameter estimated prior to grid saturation.

included forbs, geophytes, woody plants and grasses (Table 1). Although accounting for differences in species' spatial distributions substantially improved the estimated patterns of endemism and abundance, we know that not all of the species at the site were fractally distributed. As pointed out by Harte *et al.* (2001) and Lennon *et al.* (2002), if species have truly fractal distributions with different fractal dimensions, then the power-law species–area relationship cannot hold. It is, therefore, not surprising that the predicted species-level fractal model species–area relationship disagreed with the observed power-law species–area relationship.

Given that the spatial distribution of all species at the site was not truly fractal, how many species departed from fractality, and by how much? Because estimates of α_i at each spatial scale i are non-independent, we suggest a Monte Carlo approach to test for species-level self-similarity. One could simulate landscapes according to an assumed species-level self-similarity parameter α, and then use a technique similar to that presented in the Methods section, with a power-law range–area relationship as the assumed model. This approach requires having observations of a species' range-size over a sufficient range of scales before grid depletion or grid saturation. Many of the species at Little Blue Ridge reached these limits at the $A_2 = 16$ m^2 or $A_4 = 4$ m^2 spatial scale, and we had no data available at spatial scales smaller than $A_8 = 0.25$ m^2, leaving us with too few scales to rigorously test our species-level fractal model assumptions.

However, it is possible that outliers in the species-level fractal model abundance predictions (eqn 8) had non-fractal species distributions across the spatial scales $A_{13} \approx 0.008$ m^2

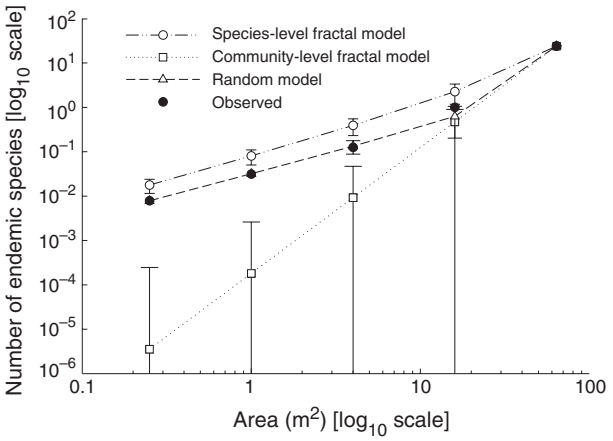

Figure 3 A comparison of the observed and predicted endemics–area relationships at Little Blue Ridge. As in Fig. 1, for each model, error bars represent 95% confidence intervals calculated from 1000 simulated landscapes; error bars smaller than symbols are not plotted. Error bars for the community-level fractal model extend to zero. At the largest sampled spatial scale, the observed data and each model agree, as they must. At smaller spatial scales, the observed data lie outside of the 95% confidence interval for both the species- and community-level fractal models (with the exception of $A_2 = 16$ m^2). The observed data and random placement model prediction are nearly indistinguishable, and lie on top of one another at every sampling area with the exception of $A_2 = 16$ m^2.

to $A_0 = 64$ m^2. Of those species with the largest deviation in their predicted and observed abundances, we looked for distinguishing characteristics that might explain departures from fractality. We found no systematic trend when considering native, exotic, serpentine endemic, annual, perrenial, dicot, or monocot species. The native forb *Plantago erecta* was by far the largest outlier (Fig. 2; Fig. 4c; observed abundance = 4827; predicted abundance = 777). This led us to consider another candidate group, *P. erecta* and four other forbs (*Microseris douglassi*, *Lasthenia californica*, *Minuartia douglasii*, *Gilia sinistra*) who had a large proportion of their individuals (>75%) in the lower left-hand (northwest) 16 m^2 quadrat of the study plot. The spatial structure of these species was possibly because of the fact that the Little Blue Ridge study plot was located on a slope with an environmental gradient very common in serpentine grasslands: deeper, alluvial soils at the foot of the slope (northwest corner), and shallow, rocky soils higher on the slope (S. Harrison, pers. comm.). This environmental gradient may have influenced the spatial distribution of water availability such that these particular forb species were only able to colonize the deeper, alluvial soils in the northwest corner of the plot. Disturbance by the western pocket gopher (*Thomomys bottae*) has been indicated as a factor influencing the spatial distribution of serpentine grassland species (Hobbs & Mooney 1991; Moloney & Levin

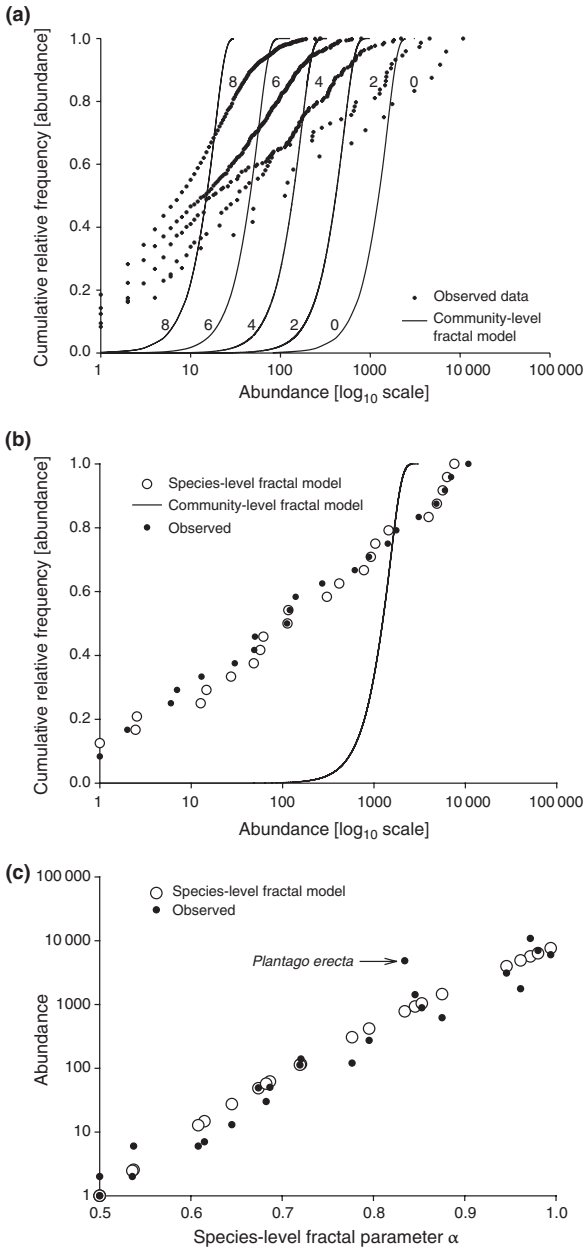

Figure 4 A comparison of the fractal model predictions and observed species abundances at Little Blue Ridge. (a) The relative cumulative frequency distribution for the community-level recursion relation and the observed species-abundance distributions at five different spatial scales ($i = 0, 2, 4, 6, 8$), indicated by the labels on the graph. (b) The relative cumulative frequency distribution for the community-level recursion relation, the observed species-abundance distributions, and the species-level fractal model predicted species-abundance distribution at spatial scale $i = 0$. (c) The observed and predicted species-level fractal model abundances vs. the estimated species-level self-similarity parameters for the 24 plant species at Little Blue Ridge. The following data points overlap: three data points at $\alpha = 0.5$ and predicted $n = 1$ and two data points at $\alpha = 0.5$ and observed $n = 1$.

1996). We noticed no gopher mounds at the study area. Moreover, the study had not been grazed since 1985 (S. Harrison, pers. comm), and we, therefore, conclude that those disturbances did not influence the spatial distribution of species at the site.

Species whose distribution may be influenced by environmental heterogeneity or other factors will not necessarily have a non-fractal spatial distribution. For a species to exhibit a fractal spatial distribution, it must have scale-invariant clustering patterns. Mechanisms such as dispersal rate, reproductive output, competitive ability, life cycle, or nutrient availability will likely influence species' spatial distributions at different spatial scales. If the suite of mechanisms that influence a species' spatial distribution result in clustering or 'occupancy' patterns that appear the same at large, intermediate, and small spatial scales, then the species will have a fractal spatial distribution. *Plantago erecta* appeared clustered at the scale of the entire study plot, yet within the northwest corner of the plot it exhibited clustering patterns that did not match the larger scale patterns. In contrast, another one of the four species with most of its individuals in the northwest corner of the plot, *L. californica*, had clustering patterns within that corner that more closely matched the larger scale patterns, and thus this species' spatial distribution appeared more fractal (Fig. 2). It is worth noting that empirical studies on serpentine substrates have found that *L. californica* has a higher seed production, a higher seed rain, and a lower survivorship of germinated seedlings in comparison with *P. erecta* (Hobbs & Mooney 1985).

The way in which the species-level fractal model endemics- and species–area relationships differ from the observed patterns provides insight into the nature of the failure of this fractal model to capture the species distributions at the site. Close examination of the endemics- and species–area relationship suggests that the species-level fractal model failed to adequately capture the clustering properties of the serpentine flora. The spatial distribution of species at the site was more aggregated than random, but less aggregated than fractal. These conclusions may be deduced from the findings of He & Legendre (2002) and Green & Ostling (in press), who showed that in a given sampling area A_i within A_0, increased regional-scale dominance (which is the converse of evenness) and increased conspecific clustering acts to decrease species richness and increase endemic species richness. Recall that the random placement model assumes the observed species-abundance distribution in A_0, and hence an identical degree of evenness as the observed ($J' = 0.63$). Likewise, the evenness predicted by the species-level fractal model ($J' = 0.66$) was nearly identical to the observed. We can, therefore, attribute the differences in the observed and predicted species- and endemics–area relationships to differences in the observed vs. modelled conspecific clustering. At each spatial scale, the random placement model overestimated species richness, and we may conclude that the spatial distribution of the individuals at the site is more aggregated than random. In contrast, the species-level fractal model underestimated species richness and overestimated endemic species richness, and we may conclude that assuming fractal species distributions and $\mu_{13} = 1$ for all species had the effect of modelling too much conspecific clustering at the site.

The question remains: why did the random placement model endemics–area relationship closely fit the observed Little Blue Ridge data? At Little Blue Ridge (and for any region), the observed and random placement model evenness must be identical. Examination of endemics–area relationships derived for a fixed species-abundance distribution at different levels of conspecific clustering (i.e. regular to random to highly aggregated) suggests that the endemics–area relationship is strongly influenced by the spatial distribution of the 'rare' species, or the species in the tail of the rank-abundance curve (Green & Ostling in press). If the intermediate and abundant species of an ecological community are not *highly* aggregated, and if the spatial distributions of species in the tail of the rank abundance curve are not significantly different from random (as were both the case at Little Blue Ridge), the observed and random placement model endemics–area relationship should closely agree. Our results suggest that a simple null model of randomly distributed individuals may serve as a practical benchmark for endemics-based extinction rate estimates across different taxa and habitat types.

One of the greatest challenges of biogeography is to develop a unified framework that quantifies the interrelationship between scaling patterns of species richness, endemism and abundance and turnover. Scaling relationships that characterize fractal species distributions have been proposed as a potential unifying framework. Our results suggest that although the community- and species-level fractal models are successful at predicting some of the observed patterns, an alternative theory is needed to link patterns in species richness, endemic species richness, and abundance. This alternative theory would ideally predict geographical patterns of ecological assemblages while accounting for differences in species spatial distributions. Such a unified theory may ultimately offer clues to the underlying mechanisms that create and constrain patterns of biodiversity.

ACKNOWLEDGEMENTS

We thank Rob Colwell, Nick Gotelli, Susan Harrison, Fangliang He, Neo Martinez, Mark Westoby, Ian Wright, and two anonymous reviewers for valuable suggestions on this manuscript. We thank Joe Callizo for expertise in plant identification and hospitality at the Pope Valley Wantrup Wildlife Preserve, Nicole Jurjavcic and Amy Wolf for help

in plant identification, and Patrick Muckleroy at Western State University for providing essential library materials. We gratefully acknowledge funding from the NSF Postdoctoral Fellowship Program to J.LG. and the Class of 1935 Endowed Chair at UC Berkeley for J.H. and A.O.

REFERENCES

Brown, J.H., Gupta, V.J., Li, B., Milne, B.T., Restrepo, C. & West, G.B. (2002). The fractal nature of nature: power-laws, ecological comlexity and biodiversity. *Philos. Trans. R. Soc. Lond. B*, 357, 619–626.

Condit, R., Hubbell, S.P., Lafrankie, J.V., Sukumar, R., Manokaran, N., Foster, R.B. & Ashton, P.S. (1996). Species-area and species-individual relationships for tropical trees: a comparison of three 50-ha plots. *J. Ecol.*, 84, 549–562.

Crawley, M.J. & Harral, J.E. (2001). Scale dependence in plant biodiversity. *Science*, 291, 864–868.

Diggle, P. (1983). *Statistical Analysis of Spatial Point Patterns*. Academic Press, London.

Finlayson, J. (1999). Species abundances across spatial scales. *Science*, 283, 1979a.

Green, J. & Ostling, A. (in press). Endemics–area relationships: the influence of species dominance and spatial aggregation. *Ecology*.

Harrison, S. (1997). How natural habitat patchiness affects the distribution of diversity in Californian serpentine chaparral. *Ecology*, 78, 1898–1906.

Harrison, S. (1999a). Local and regional diversity in a patchy landscape: native, alien, and endemic herbs on serpentine. *Ecology*, 80, 70–80.

Harrison, S. (1999b). Native and alien species diversity at the local and regional scales in a grazed California grassland. *Oecologia*, 121, 99–106.

Harrison, S. & Inouye, B.D. (2002). High beta diversity in the flora of Californian serpentine 'islands'. *Biodiv. Conserv.*, 11, 1869–1876.

Harrison, S., Inouye, B.D. & Safford, H.D. (2003). Ecological heterogeneity in the effects of grazing and fire on grassland diversity. *Conserv. Biol.*, 17, 837–845.

Harte, J. & Kinzig, A.P. (1997). On the implications of species-area relationships for endemism, spatial turnover, and food web patterns. *Oikos*, 80, 417–427.

Harte, J., Kinzig, A. & Green, J. (1999a). Self-similarity in the distribution and abundance of species. *Science*, 284, 334–336.

Harte, J., McCarthy, S., Taylor, K., Kinzig, A. & Fischer, M.L. (1999b). Estimating species–area relationships from plot to landscape scale using species spatial-turnover data. *Oikos*, 86, 45–54.

Harte, J., Blackburn, T. & Ostling, A. (2001). Self-similarity and the relationship between abundance and range size. *Am. Nat.*, 157, 374–386.

He, F. & Gaston, K.J. (2000). Estimating species abundance from occurrence. *Am. Nat.*, 156, 553–559.

He, F. & Legendre, P. (2002). Species diversity patterns derived from species-area models. *Ecology*, 83, 1185–1198.

Hickman, J.C. (1993). *The Jepson Manual: Higher Plants of California*. University of California Press, Berkeley, CA.

Hobbs, R.J. & Mooney, H.A. (1985). Community and population dynamics of serpentine grassland annuals in relation to gopher disturbance. *Oecologia*, 67, 342–351.

Hobbs, R.J. & Mooney, H.A. (1991). Effects of rainfall variability and gopher disturbance on serpentine annual grassland dynamics. *Ecology*, 72, 59–68.

Kinzig, A.P. & Harte, J. (2000). Implications of endemics–area relationships for estimates of species extinctions. *Ecology*, 81, 3305–3311.

Kruckeberg, A.R. (2002). *Geology and Plant Life – The Effects of Landforms and Rock Types on Plants*. University of Washington Press, Seattle.

Kunin, W.E. (1998). Extrapolating species abundance across spatial scales. *Science*, 281, 1513–1515.

Kunin, W.E., Hartley, S. & Lennon, J.J. (2000). Scaling down: On the challenge of estimating abundance from occurrence patterns. *Am. Nat.*, 156, 560–566.

Lennon, J.J., Kunin, W.E. & Hartely, S. (2002). Fractal species distributions do not produce power-law species–area relationships. *Oikos*, 97, 378–386.

Milne, B.T. (1997). Applications of fractal geometry in wildlife biology. In: *Wildlife and Landscape Ecology: Effects of Pattern and Scale* (ed. Bissonette, J.A). Springer, New York, pp. 32–69.

Moloney, K.A. & Levin, S.A. (1996). The effects of disturbance architecture on landscape-level population dynamics. *Ecology*, 77, 375–394.

Ostling, A., Harte, J., Green, J.L. & Kinzig, A.P. (in press). A community-level fractal property produces power-law species–area relationships. *Oikos*.

Pielou, E.C. (1975). *Ecological Diversity*. John Wiley and Sons, Inc., New York.

Plotkin, J.B. (2000). Species-area curves, spatial aggregation, and habitat specialization in tropical forests. *J. Theor. Biol.*, 207, 81–99.

Plotkin, J.B., Potts, M.D., Yu, D.W., Bunyavejchewin, S., Condit, R., Foster, R., Hubbell, S., LaFrankie, J., Manokaran, N., Seng, L.H., Sukumar, R., Nowak, M.A. & Ashton, P.S. (2000). Predicting species diversity in tropical forests. *Proc. Natl Acad. Sci. U S A*, 97, 10850–10854.

Ritchie, M.E. & Olff, H. (1999). Spatial scaling laws yield a synthetic theory of biodiversity. *Nature*, 400, 557–560

Rosenzweig, M.L. (1995). *Species Diversity in Space and Time*. Cambridge University Press, Cambridge.

University of California-Davis Natural Reserve System (UCD-NRS). (2003). Natural history of the McLaughlin Reserve, Napa, Lake and Yolo Counties, CA. Available at URL http://nrs.ucop.edu/reserves/mclaughlin.html

Whittaker, R.H. (1954). The vegetational responses to serpentine soils. *Ecology*, 35, 275–288.

Whittaker, R.H. (1960). Vegetation of the Siskiyou Mountains, Oregon and California. *Ecol. Monogr.*, 30.

Wolf, A. (2001). Conservation of endemic plants in serpentine landscapes. *Biol. Conserv.*, 100, 35–44.

Zar, J.H. (1999). *Biostatistical Analysis*, 4th edn. Prentice Hall, Inc., London.

Editor, Pablo Marquet
Manuscript received 22 May 2003
First decision made 27 June 2003
Manuscript accepted 12 August 2003